Repression of tumor suppressor miR-451 is essential for NOTCH1-induced oncogenesis in T-ALL

Xiaoyu Li,[1] Takaomi Sanda,[2] A. Thomas Look,[2] Carl D. Novina,[1] and Harald von Boehmer[1]

[1]Department of Cancer Immunology and AIDS and [2]Department of Pediatric Oncology, Dana-Farber Cancer Institute, Harvard Medical School, Boston, MA 02215

The NOTCH1 signaling pathway is a critical determinant of cell fate decisions and drives oncogenesis through mechanisms that are incompletely understood. Using an established mouse model of T cell acute lymphoblastic leukemia (T-ALL), here we report that induction of intracellular Notch1 (ICN1) leads to repression of miR-451 and miR-709. ICN1 decreases expression of these miRNAs by inducing degradation of the E2a tumor suppressor, which transcriptionally activates the genes encoding miR-451 and miR-709. Both miR-451 and miR-709 directly repress Myc expression. In addition, miR-709 directly represses expression of the Akt and Ras-GRF1 oncogenes. We also show that repression of miR-451 and miR-709 expression is required for initiation and maintenance of mouse T-ALL. miR-451 but not miR-709 is conserved in humans, and human T-ALLs with activating *NOTCH1* mutations have decreased miR-451 and increased MYC levels compared with T-ALLs with wild-type *NOTCH1*. Thus, miR-451 and miR-709 function as potent suppressors of oncogenesis in NOTCH1-induced mouse T-ALL, and miR-451 influences MYC expression in human T-ALL bearing *NOTCH1* mutations.

CORRESPONDENCE
Harald von Boehmer:
Harald_von_boehmer@dfci.harvard.edu
OR
Carl D. Novina:
carl_novina@dfci.harvard.edu

Abbreviations used: ChIP, chromatin immunoprecipitation; ICN1, intracellular Notch1; miRNA, micro RNA; T-ALL, T cell acute lymphoblastic leukemia; UTR, untranslated region.

NOTCH1 is a transcriptional activator with an essential role in the formation of numerous cancers. In human T cell acute lymphoblastic leukemia (T-ALL), NOTCH1 is frequently activated by mutation and contributes to molecular pathogenesis as a dominant oncogene. Several essential pathways of NOTCH1-driven oncogenesis have been described. The human *NOTCH1* gene was originally cloned in T-ALL at the breakpoint of the t(7;9) chromosomal translocation, which places the *NOTCH1* gene under the control of the *TCR*β gene promoter (Ellisen et al., 1991). Although this translocation occurs in only a small percentage of primary T-ALL, activating mutations in the *NOTCH1* gene have been identified in >50% of patients with this disease (Weng et al., 2004). Several other alterations that result in increased intracellular Notch1 (ICN1) levels after proteolytic cleavage have also been identified (Pece et al., 2004; O'Neil et al., 2007). *MYC* has been identified as a critical direct downstream target gene of NOTCH1 in leukemogenesis (Palomero et al., 2006; Sharma et al., 2006; Weng et al., 2006), but mouse T-ALL studies suggest that NOTCH1 has additional unidentified targets in transformation (Girard et al., 1996). In addition, numerous tumor suppressors and oncogenes have been identified that cooperate with NOTCH1 in multiple distinct pathways, leading to transformation in human T-ALL. Undoubtedly, many more examples of cooperating mutations will be discovered (Armstrong and Look, 2005).

For our studies, we capitalized on a widely used mouse model of T-ALL (Pear et al., 1996) to search for molecular mechanisms downstream of activated Notch1. ICN1 overexpression in mouse hematopoietic precursor cells results in T-ALL characterized by extensively dysregulated gene expression in the face of genomic stability (Li et al., 2008). In this model, *Lin*-negative BM cells are retrovirally transduced with ICN1 before transfer into γ-irradiated recipients (Pear et al., 1996). ICN1 overexpression first generates nontumorigenic $CD4^+CD8^+$ $TCR\alpha\beta^+$

The Rockefeller University Press $30.00
J. Exp. Med. Vol. 208 No. 4 663-675
www.jem.org/cgi/doi/10.1084/jem.20102384

The Journal of Experimental Medicine

cells with polyclonal *TCR*β chain rearrangements, followed by tumorigenic $CD4^+CD8^+$ cells with monoclonal *TCR*β chain rearrangement paired with diverse *TCR*α chains. Thus, malignant transformation follows pre-TCR signaling but sets in before termination of TCRα rearrangement (Li et al., 2008), and mice develop overt T-ALL between 6 and 8 wk after BM transplantation. Several genes regulating the development and proliferation of immature T cells, including Myc, Akt, and Ras-GRF1, are specifically up-regulated in ICN1-overexpressing T-ALL tumor cells (Li et al., 2008). These appear to be critical in oncogenesis, because Myc is an essential oncogenic pathway downstream of Notch1 (Palomero et al., 2006; Sharma et al., 2006; Weng et al., 2006; Li et al., 2008), and Akt and Ras-GRF1 are components of cooperating oncogenic pathways in human T-ALL (Lübbert et al., 1990; Palomero et al., 2007; Gutierrez et al., 2009). Thus, in terms of elevated oncogene expression mouse T-ALL resembles human T-ALL in spite of its genomic stability because (a) >50% of human T-ALL cases have mutationally activated NOTCH1 and overexpress ICN1 (Weng et al., 2004); (b) ICN1 directly regulates Myc by binding to regulatory sequences in the *Myc* promoter (Palomero et al., 2006); (c) ICN1-mediated activation of Myc is required to maintain leukemic growth (Palomero et al., 2006; Sharma et al., 2006; Weng et al., 2006); (d) mouse and human ICN1 increases PI3K/Akt activity and prolongs the survival of leukemic cells (Sade et al., 2004; Palomero et al., 2007; Gutierrez et al., 2009); and (e) the overall patterns of NOTCH1-mediated gene expression in human and mouse T-ALLs are remarkably similar (Sanda et al., 2010). Thus, the majority of human T-ALLs with *NOTCH1* gene mutations share many features in common with the ICN1-induced mouse model, including dysregulated Myc and Akt expression and repression of cell cycle inhibitors.

Because mouse ICN1-induced T-ALL displays globally altered gene expression in spite of genomic stability (Li et al., 2008), we considered the possibility that altered expression of micro RNAs (miRNAs) might be an important contributor to malignant transformation of T cells. miRNAs are known to affect developmental transitions in T cells (Li et al., 2007), and aberrantly expressed miRNAs have been shown to play important roles in malignant transformation in other tumor types. For example, increased expression of specific miRNAs such as miR-17–92 cluster drives leukemogenesis in mice (He et al., 2005; O'Donnell et al., 2005), indicating that miRNAs could function as oncogenes (oncomirs). Indeed, a novel activating translocation affecting the miR-17–92 cluster was recently described that coincides with a rearrangement that activates Notch1 (Mavrakis et al., 2010). Increased miR-19 was shown to act through multiple negative regulators of the PI3 kinase pathway.

Conversely, miRNAs may function as tumor suppressors, although it has been more difficult to causally connect miRNA inactivation to tumor initiation. Recent studies indicate tumor suppressive functions during maintenance and metastasis. In the best example, let-7 is considered a tumor suppressor miRNA, because its expression is reduced in numerous cancers (Takamizawa et al., 2004; Lu et al., 2005; Volinia et al., 2006), its reduced expression correlates with poor patient outcomes (e.g., lung cancer; Takamizawa et al., 2004), and let-7 normally represses the expression of RAS, including its oncogenic forms (Johnson et al., 2005). Additionally, transduction of let-7 reduces lung tumor growth in mice (Ortholan et al., 2009). Here, we report reduced tumor suppressor miRNA activity that is required for tumor initiation. We identified two miRNAs, miR-451 and miR-709, which are transcriptional targets of the E2a tumor suppressor, which is degraded upon ICN1 induction in mouse T-ALL cells. We report a cooperative loop in which miR-451 and miR-709 must be down-regulated for initiation and maintenance of ICN1-induced T-ALL and which together directly target and reduce the expression levels of several oncogenes, such as Myc, Akt, and Ras-GRF1.

RESULTS

Reduced miR-451 and miR-709 up-regulate Myc, Akt, and Ras-GRF1

To elucidate tumorigenic pathways that cooperate with activated Notch1 in leukemogenesis in the absence of detectable genomic alterations, we performed miRNA expression profiling of normal $CD4^+CD8^+$ thymocytes; benign, polyclonal,

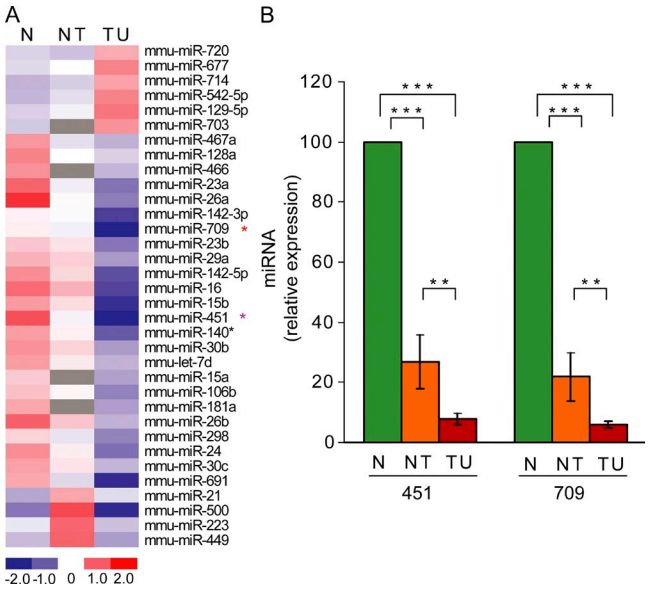

Figure 1. miR-451 and miR-709 are robustly reduced in T-ALL. (A) Hierarchical clustering of differentially expressed miRNA genes in normal $CD4^+CD8^+$ thymocytes (N), nonmalignant ICN1-overexpressing $CD4^+CD8^+$ cells (NT), and T-ALL tumor $CD4^+CD8^+$ cells (TU) detected by LNA-based miRNA expression profiling. Red denotes up-regulated expression and blue denotes down-regulated expression. The scale is $\log_2$. Asterisks indicate miR-451 and miR-709. (B) Independent validation of down-regulated expression miR-451 and miR-709 by qRT-PCR in N, NT, and TU. RNU6B was used as an endogenous control to normalize expression. **, $P < 0.01$; ***, $P < 0.001$. Relative expression (%) compared with N was calculated. Data are shown as mean ± SD for triplicate experiments. The large dynamic range of the qRT-PCR assay likely accounts for the very large reduction in expression detected in this assay compared with microarray expression profiling in Fig. 1 A.

$CD4^+CD8^+$ ICN1-overexpressing cells, and malignant, monoclonal T-ALL cells (Fig. 1 A). Microarray analysis revealed several consistently dysregulated miRNAs during the progression of the leukemogenesis, including the known tumor suppressor miRNAs let-7d (Takamizawa et al., 2004; Johnson et al., 2005; Lu et al., 2005; Volinia et al., 2006; Lee and Dutta, 2007), miR-15a, and miR-16 (Bonci et al., 2008; Calin et al., 2005; Cimmino et al., 2005), as well as miR-451 and miR-709, which have not previously been linked to T-ALL oncogenesis. Both miR-451 and miR-709 are dynamically regulated during normal T cell development (Fig. S1 A) and are progressively down-regulated during T-ALL transformation first in benign polyclonal cells and further in malignant monoclonal cells (Fig. 1 B), suggesting that they function as tumor suppressors.

Because miR-451 and miR-709 demonstrated the most robust differential expression (and a consistent trend of down-regulation)—transitioning from normal thymocytes (N), to benign polyclonal (NT), to malignant monoclonal tumor (TU) samples—and because these were previously uncharacterized miRNAs, we pursued these two miRNAs for further analysis. We used computational algorithms (Lewis et al., 2003; John et al., 2004) to predict the targets of miR-451 and miR-709. We identified the Myc oncogene as a potential target of both miRNAs, and the Akt and Ras-GRF1 oncogenes as potential targets of miR-709 (Fig. 2 A). Myc is known to be a direct and essential target of the Notch1-containing transcriptional complex in the pathogenesis of both human and mouse T-ALL (Palomero et al., 2006; Sharma et al., 2006; Weng et al., 2006), but it is unclear whether transcriptional activation by ICN1 is sufficient for malignant transformation. An attractive hypothesis is that miR-451 and miR-709 are down-regulated as a mean to potentiate ICN1-induced overexpression of Myc.

To experimentally validate these predictions, we reconstituted miR-451 and miR-709 by transfection (Fig. S2) or retroviral infection (Fig. 2 B and Fig. 3) of T-ALL cells back to physiological levels found in normal $CD4^+CD8^+$ thymocytes (compare Fig. S2 and Fig. 3 B with Fig. 1 B) and examined Myc, Akt,

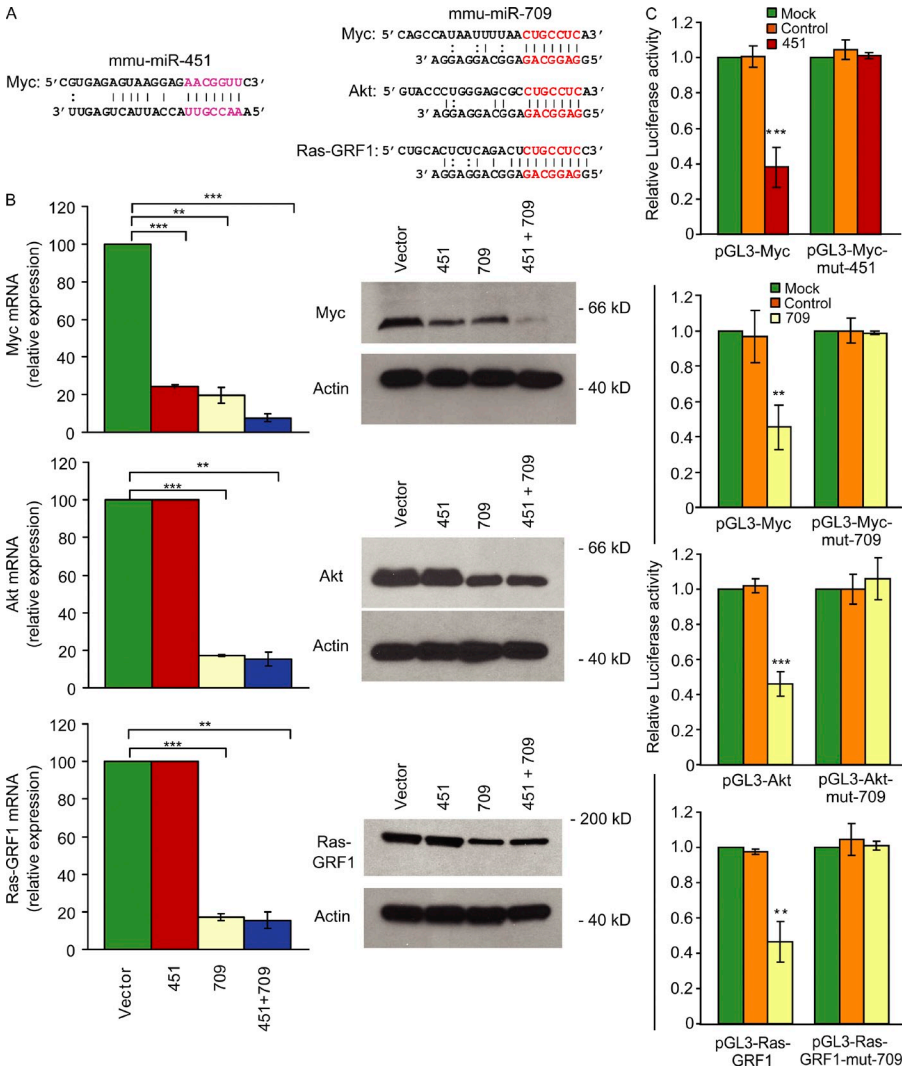

Figure 2. miR-451 and miR-709 repress Myc; miR-709 also represses Akt and Ras-GRF1. (A) Computationally-predicted miRNA–mRNA interactions between miR-451 and the 3′UTR of Myc (15–21) miR-709, and the 3′UTR of Myc (125–132), miR-709 and the 3′UTR of Akt (670–677), miR-709 and the 3′UTR of Ras-GRF1 (180–187); all miRNA binding sites were predicted by TargetScan (Lewis et al., 2003). The miR-709 binding site in the 3′UTR of Myc was also predicted by MIRANDA (John et al., 2004). (B) Expression of miR-451 and miR-709 at physiological levels (demonstrated in Fig. 3 B) represses target mRNA and protein levels in T-ALL tumor cells. Quantitative analysis of Myc, Akt, and Ras-GRF1 mRNA expression (left) and protein expression (right) in T-ALL tumor cells infected with retroviruses expressing no miRNA (Vector), miR-451 (451), miR-709 (709), or both (451+709) as indicated. GAPDH mRNA was used as control for mRNA expression. Relative mRNA expression (%) compared with Vector was calculated. Data are shown as mean ± SD for triplicate experiments. **, $P < 0.01$; ***, $P < 0.001$. β-Actin was used as loading control in Western blotting (right). (C) Firefly luciferase constructs possessing WT 3′UTRs (pGL3-Myc, pGL3-Akt, and pGL3-Ras-GRF1) or point mutant 3′UTRs (corresponding to seed region of miR-451 and miR-709) of Myc, Akt, or Ras-GRF1 (pGL3-Myc-mut-451, pGL3-Myc-mut-709, pGL3-Akt-mut-709 and pGL3-Ras-GRF1-mut-709) were co-transfected with renilla luciferase constructs into NIH-3T3 cells alone (Mock), with a nonspecific control (Control), or with a miR-451 or miR-709. Firefly luciferase activity was normalized to renilla luciferase activity. Relative luciferase activity compared with Mock is shown. **, $P < 0.01$, ***, $P < 0.001$. Data are shown as mean ± SD for triplicate experiments.

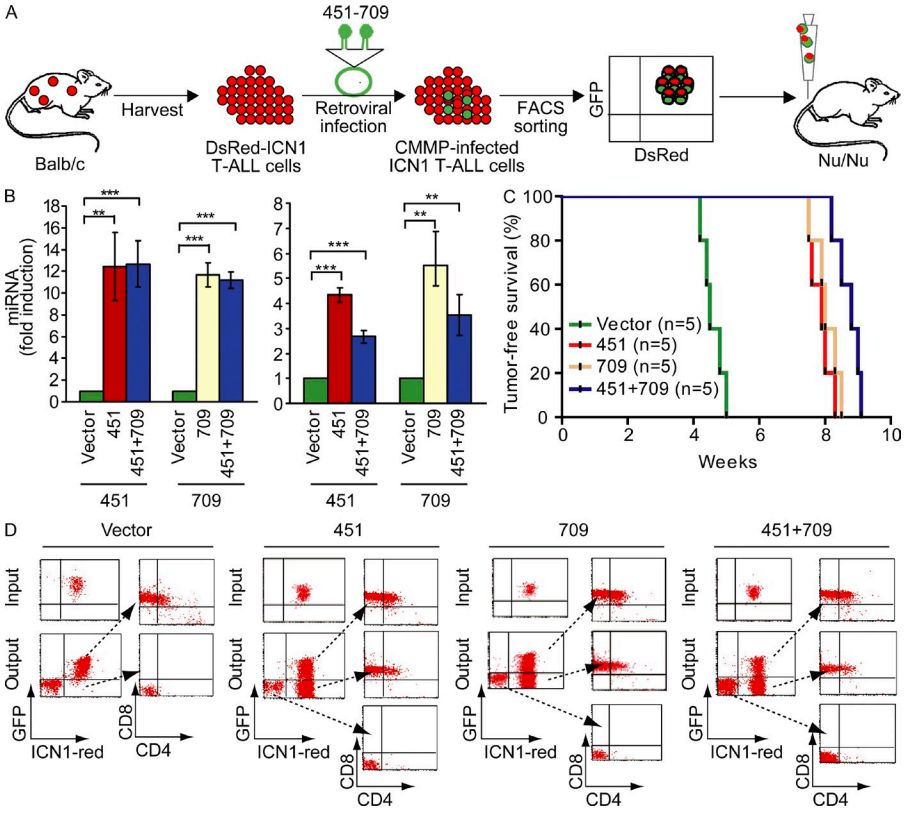

Figure 3. Physiological expression of miR-451 and miR-709 slows T-ALL tumor growth in vivo. (A) Schematic representation of the experimental design. ICN1-induced T-ALL formation was initiated by transplantation of BM cells transduced with MSCV retrovirus encoding ICN1-DsRed into BALB/c mice. ICN1-DsRed–overexpressing T-ALL cells were harvested and infected with a CMMP retrovirus vector encoding GFP without or with miR-451, miR-709, or both. DsRed$^+$GFP$^+$ cells were then sorted by FACS and transplanted into Nu/Nu recipient mice. (B) Expression of miR-451 and miR-709 in the T-ALL cells infected without (Vector) or with miR-451 (451), miR-709 (709), or both (451+709) were assessed by miRNA quantitative RT-PCR before adoptive transfer (left) or after tumor formation (right). RNU6B was used as an endogenous small RNA control to normalize miRNA expression. Fold induction compared with Vector was determined. Data are shown as mean ± SD for triplicate experiments. **, $P < 0.01$; ***, $P < 0.001$. (C) Kaplan-Meier analysis of survival time of Nu/Nu recipients in each group is shown. $P < 0.01$ (Vector vs. 451); $P < 0.01$ (Vector vs. 709); and $P < 0.01$ (Vector vs. 451+709). (D) FACS analysis of miR-451 and/or miR-709 (GFP) and ICN1 (DsRed), as well as CD4 and CD8 expression in T-ALL tumor cells after infection and FACS sorting before adoptive transfer (Input) or after tumor formation (Output).

and Ras-GRF1 mRNA and protein levels. Our data indicate that we achieved near physiological reconstitution of miR-451 or miR-709, which repressed Myc at the mRNA and protein levels, and that these two miRNAs acted synergistically to reduce Myc levels when coexpressed in T-ALL cells. In addition, reconstitution of miR-709, but not miR-451, repressed Akt and Ras-GRF1 mRNA and protein levels (Fig. 2 B and Fig. S2 D).

To experimentally define the miR-451 and miR-709 binding sites in the 3′ untranslated regions (3′UTRs) of the predicted target genes, we cloned WT or point mutant versions of the Myc, Akt, or Ras-GRF1 3′UTR gene segments into firefly luciferase reporter vectors and performed dual luciferase assays upon reconstitution of miR-451 and miR-709 (Fig. 2 C). Co-transfection of miR-451 or miR-709, but not a control miRNA, specifically decreased expression of firefly luciferase reporter mRNAs possessing the WT Myc 3′UTR. When the predicted seed region binding sequences in the Myc 3′UTR were mutated, firefly luciferase expression returned to baseline levels, implicating these sequences in miRNA binding. Similarly, co-transfection of miR-709 but not control miRNA specifically decreased firefly luciferase activity in reporter mRNAs possessing WT Akt and Ras-GRF1 3′UTRs, but not miR-709 seed region binding sequence point mutant 3′UTRs. These mutants in miR-451 or miR-709 binding sites completely are resistant to miR-451– and miR-709–mediated repression, and provide further evidence that Myc is a genuine target of miR-451 and miR-709 and that Akt and Ras-GRF1 are genuine targets of miR-709.

Reduction of miR-451 and miR-709 is essential for maintenance of T-ALL

To study the function of miR-451 and miR-709 in T-ALL leukemogenesis, we expressed physiological levels (compared with normal CD4$^+$CD8$^+$ thymocytes; Fig. 1 B) of these miRNAs in ICN1-transduced T-ALL cells and adoptively transferred these cells into nude mice. Co-transfection (Fig. S2) or retroviral expression (Fig. 3) of miR-451 and miR-709 into ICN1-induced T-ALL cells delayed tumor development compared with controls (Fig. 3 C and Fig. S2 C). At 48 h after transfection or retrovirus infection, the levels of miR-451 and miR-709 approximated the levels of these miRNAs in normal CD4$^+$CD8$^+$ thymocytes (Fig. 1 B). miRNA-targeted oncoprotein levels (Myc, Akt, and Ras-GRF1; Fig. 2 B) and the levels of miR-451 and miR-709 were measured after introduction of the miRNA (Fig. 3 B, left, and Fig. S2 B) and at the time that overt T-ALL developed in the mouse (Fig. 3 B, right), showing that reconstitution of these miRNAs to physiological levels delayed the growth of ICN1-induced tumor cells. miR-451 and miR-709 are expressed from the same transcript as GFP, and miRNA expression is directly correlated with GFP expression (Fig. S1 B). The tumors that eventually developed contained a large proportion of cells that lost GFP expression (Fig. 3, C and D). The control vector did not result in a loss of GFP expression, indicating that the expression of the miRNAs inhibited tumor growth. Thus, T-ALL

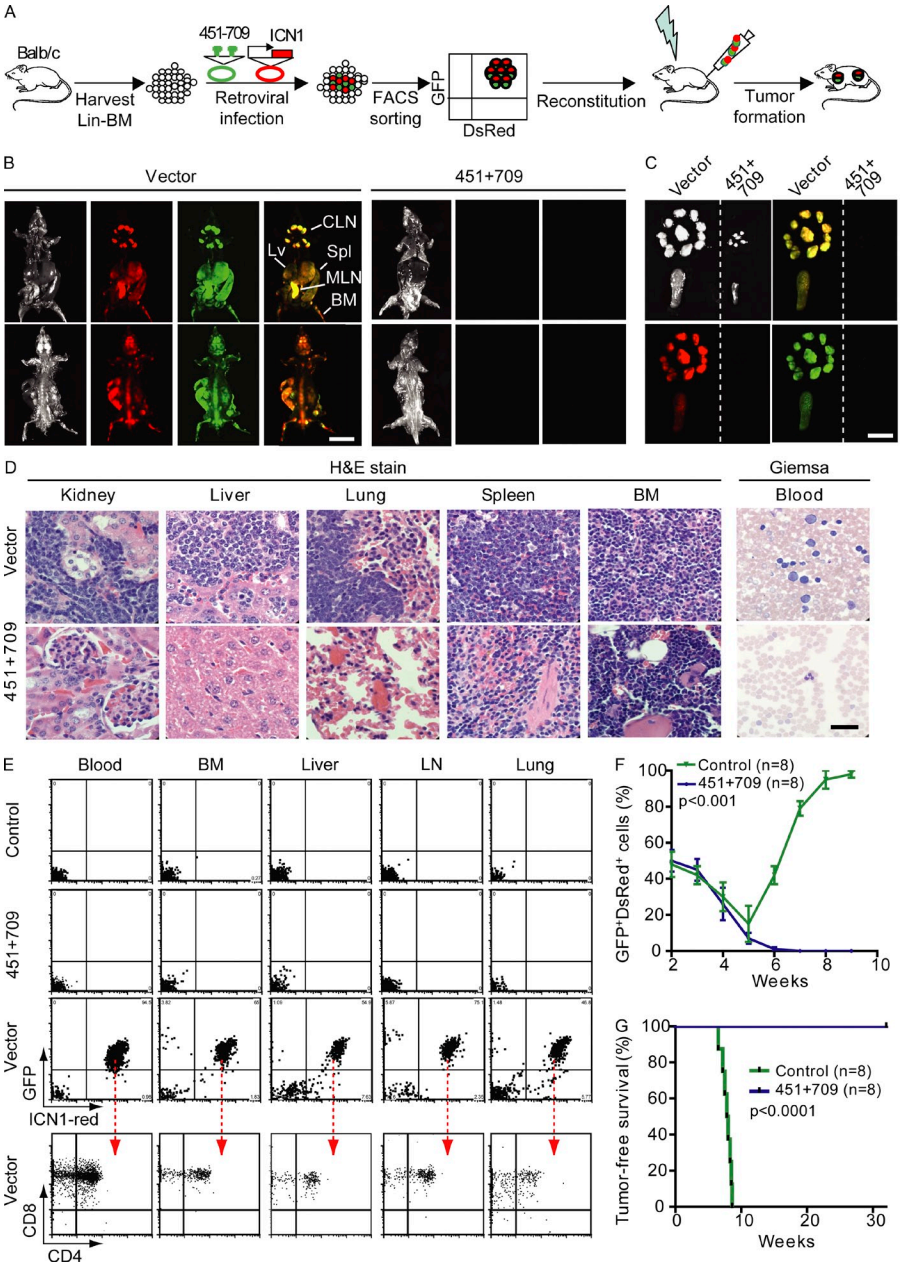

Figure 4. Coordinate expression of miR-451 and miR-709 blocks ICN1-induced tumor initiation in vivo. (A) Schematic representation of the experimental design. Lin$^-$ BM cells harvested from BALB/c mice were infected with a retrovirus expressing DsRed and ICN1 and with a retrovirus expressing GFP with or without miR-451 and miR-709. DsRed$^+$GFP$^+$ cells were sorted by FACS and adoptively transferred into sublethally irradiated (lightning bolt) syngeneic mice. T-ALL was assessed at 6 wk after BM transplantation. (B) Whole-body imaging of mice expressing ICN1-DsRed (red) and GFP (green) without (Vector, left) or with miR-451 and miR-709 (451+709, right) are shown. Bar, 25 mm. (C) LNs and spleens harvested from Vector and 451+709 recipients are shown. Bar, 15 mm. (D) Hematoxylin and eosin (H&E) staining to detect tumor infiltrates in kidney, liver, lung, spleen, and BM of recipients of BM cells transduced with vector or miR-451 and miR-709 (451+709). Blood smears were assessed by Giemsa staining (right panel). Scale bar, 10 µm. (E) FACS analysis of DsRed$^+$GFP$^+$ cells in blood, BM, liver, LN, or lung after transplantation of BM cells. BM cells transduced with neither ICN1-DsRed nor miR-451-miR-709-GFP are shown as a control. CD4 and CD8 expression on the DsRed$^+$GFP$^+$ cells from control mice were also analyzed. (F) Percentage of DsRed$^+$GFP$^+$ cells in the blood at indicated times after BM transplantation ($n = 8$ in each group, $P < 0.001$). (G) Kaplan-Meier analysis of survival time in each group ($n = 8$) is shown. $P < 0.0001$ by log-rank test.

outgrowth results from selection against the cells with increased miR-451 and miR-709 expression. The CD4/CD8 staining in the second column shows that all tumor cells exhibited the same CD4/CD8 expression profile. Collectively, our data show that physiological levels of miR-451 and miR-709 are sufficient to repress the expression levels of Myc, Akt, and Ras-GRF1 and that repression by these miRNAs accelerates tumor cell growth during ICN1-induced T-ALL oncogenesis.

Reduction of miR-451 and miR-709 is essential for initiation of T-ALL

To identify potential roles for miR-451 and miR-709 as tumor suppressors during the initiation of T-ALL by ICN1, we co-infected *Lin*-negative normal mouse BM cells with a retrovirus expressing ICN1 together with DsRed and a retrovirus expressing physiological levels of miR-451 and miR-709 together with GFP. The infected cells were injected into sublethally irradiated recipients (Fig. 4 A). Expression of ICN1-DsRed and the GFP vector control led to widespread tumor formation in several tissues, including liver, spleen, BM, and multiple LNs as determined by whole body (Fig. 4 B) and lymphoid organ imaging (Fig. 4 C), histopathology (Fig. 4 D and Fig. S3 B), FACS analysis (Fig. 4 E), and immunohistochemistry (Fig. S3, C and D). In contrast, ectopic expression of miR-451 and miR-709 completely blocked tumor formation in any site by any of these metrics. Moreover, the spleens and LNs harvested from mice expressing miR-451 and miR-709 were normal compared with organs from tumor-bearing mice, which were grossly enlarged (Fig. 4 C). FACS analysis of LNs, BM, lung, and livers harvested from mice infected with the empty vector control demonstrated numerous GFP$^+$DsRed$^+$ tumor cells composed mostly of CD4$^+$CD8$^+$ cells and CD4$^-$CD8$^+$ cells,

as shown by CD4/CD8 staining (Fig. 4 E, bottom row) consistent with ICN1-induced T-ALL (Li et al., 2008). In contrast, mice expressing miR-451 and miR-709 contained no detectable tumor cells. During the early stages after BM transplantation, DsRed$^+$GFP$^+$ cells are present in both of control mice and miR-451+miR-709 mice, reflecting a polyclonal and nontumorigenic stage (Li et al., 2008); however, at later stages after bone marrow transplantation, DsRed$^+$GFP$^+$ cells expanded rapidly only in the mice expressing the control vector, indicating outgrowth of monoclonal T-ALL tumors. No DsRed$^+$GFP$^+$ cells could be detected at 6–8 wk after transplantation of BM cells expressing miR-451+miR-709 (Fig. 4 F and Fig. 4 G). It is important to emphasize that these mice exhibited normal thymic development and generated nonmalignant ICN1 overexpressing CD4$^+$CD8$^+$ cells in peripheral lymphoid tissue. Thus, the expression of miRNAs at levels found in normal thymocytes specifically inhibits malignant transformation after pre-TCR signaling. The absence of tumor cells in the BM, normal thymic development, and the appearance of comparable numbers of nonmalignant (predominantly CD4$^+$CD8$^+$) GFP$^+$DsRed$^+$ cells in peripheral tissues 3 wk after BM transplantation (Fig. S4) indicates that the combined expression of ICN1 and miR-451 and miR-709 did not simply block T cell differentiation or migration. Together, these data indicate that miR-451 and miR-709 are tumor suppressors whose expression must be down-regulated during ICN1-induced T-ALL transformation.

miR-451 and miR-709 are E2a transcriptional target genes

To investigate the mechanism of reduced miR-451 and miR-709, we performed miRNA-specific RT-PCR. ICN1 induction led to reduced expression of primary (pri-miRNAs), premature (premiRNAs), and mature forms of both miR-451 and miR-709 (unpublished data), arguing against posttranscriptional down-regulation of these miRNAs. To test for a mechanism of transcriptional down-regulation, we examined promoter regions of these genes and noted 4 E-box binding motifs (CANNTG) in the miR-451 promoter and 2 E-box binding motifs in the miR-709 promoter (Fig. 5 A). Because (a) E2a-encoded proteins are essential for B cell and T cell development (Bain et al., 1994; Zhuang et al., 1994; Ikawa et al., 2006); (b) E2a-defieient mice regularly develop T-ALL (Bain et al., 1997); and (c) E2a proteins are rapidly degraded in ICN1-induced T-ALL (Li et al., 2008), we examined transcriptional regulation of miR-451 and miR-709 by E2a.

Chromatin immunoprecipitation (ChIP) for normal CD4$^+$CD8$^+$ thymocytes using an anti-E2a antibody demonstrated a 25-fold enrichment of the miR-451 promoter and a 15-fold enrichment of the miR-709 promoter compared with controls (Fig. 5 B) demonstrating that endogenous E2a occupies these miRNA promoters in normal thymocytes. To determine whether E2a transcriptionally activates these promoters through binding to E-box motifs, we cloned WT or E-box deletion mutant miR-451 or miR-709 promoters into luciferase-expressing constructs and measured luciferase activity when co-transfected with E47, one of splice forms of E2a. Our data clearly indicate E47-dependent activation of WT but not E-box mutant miR-451 and miR-709 promoters (Fig. 5 C). T-ALL cells normally have very little E2a protein (Li et al., 2008,) and thus the effect of an E2a knockdown cannot be studied in these cells. Instead, to functionally link E2a activation to miR-451 and miR-709 expression in T-ALL, we ectopically expressed E2a. ICN1-DsRed tumor cells were transduced with the empty retroviral vector or retroviral construct encoding a nondegradable mutant form E47 (Fig. 5 D). Restoration of E47 significantly induced miR-451 and miR-709 expression in the ICN1 tumor cells (Fig. 5 E) and reduced ICN1-tumor cell growth (Fig. 5 F) compared with cells transduced with retroviral empty vector controls. Together, these data demonstrate that miR-451 and miR-709 are direct transcriptional targets of E2a and indicate a mechanism of Notch1-dependent suppression of these miRNAs leading to derepression of T-ALL oncogenes (Fig. 5 G).

NOTCH1 mutant human T-ALL exhibit decreased miR-451 and increased Myc

To address the question whether reduced miRNA expression could also contribute to human T-ALL, we examined human miR-451 (humans lack a miR-709 homologue) and its target MYC levels in human T-ALLs that have been segregated into groups based upon activating *NOTCH1* mutation status, as well as in normal human thymocytes (Fig. 6 A). The characteristics of these primary T-ALL patient samples and cell lines are listed in Table S1. We identified lower miR-451 expression levels in primary samples harboring activating *NOTCH1* mutations (middle) and T-ALL cell lines expressing the ICN1 protein (right), when compared with patient samples that lacked *NOTCH1* gene mutations (left) or normal thymocytes (control; Fig. 6 A). The MYC levels were significantly higher in T-ALL cell lines expressing the ICN1 than in primary patient samples lacking activating *NOTCH1* mutations. Importantly, analysis of cell surface marker expression did not indicate any correlation between cell differentiation stage and miR-451 expression, suggesting that maturational arrest alone did not explain these differences (Table S1). These data indicate that miR-451 is selectively reduced in T-ALLs exhibiting mutational activation of NOTCH1, suggesting that miR-451 functions as a tumor suppressor in NOTCH1-driven human and mouse T-ALL.

We also analyzed the expression levels of miR-451 and MYC in a panel of established human T-ALL cell lines. We previously reported that ICN1 is constitutively overexpressed in most of the T-ALL cell lines, as a result of genetic mutations of *NOTCH1* and/or *FBXW7* (O'Neil et al., 2007; see Table S1 for ICN1 expression and genetic status of *NOTCH1* and *FBXW7* in the 11 T-ALL cell lines). All of the ICN1-positive T-ALL cell lines demonstrated very low levels of miR-451 and expressed increased levels of MYC (Fig. 6 A), presumably reflecting selection for T-ALL cells with very high MYC levels and proliferative rates during their establishment and maintenance in tissue culture. Computational analysis predicted that human miR-451 also targets the human MYC

mRNA (Fig. 6 B). Transfection of miR-451 specifically decreased expression of firefly luciferase reporter mRNAs possessing the WT MYC 3′UTR, but not mutated 3′UTR (Fig. 6 C), indicating that MYC is a direct target of miR-451.

To mechanistically link altered miR-451 expression to the biology of human T-ALL, we transduced miR-451 and the empty GFP vector into four representative ICN1$^+$ human T-ALL cell lines (Fig. S5), which are characterized by very low miR-451 expression levels (Fig. 6 A). Expression of miR-451 on its own was not sufficient to inhibit the growth of these T-ALL cell lines (Fig. S5 B). Because miR-451 acts synergistically with activated NOTCH signaling in mouse T-ALL, we analyzed the effect of programmed expression of miR-451 in human T-ALL cell lines when combined with inhibition of NOTCH1 signaling using a γ-secretase inhibitor (GSI, MRK-003), a derivative of which is currently used in clinical trials of T-ALL (Paganin and Ferrando, 2011). We and others have previously reported that GSI treatment down-regulates MYC and inhibits T-ALL cell growth (Palomero et al., 2006; Sharma et al., 2006; Weng et al., 2006). In this experiment, MYC levels were reduced in each of the four cell lines overexpressing miR-451 compared with controls (Fig. 6 D, green bars), and MYC levels were further down-regulated after GSI treatment for each cell line (Fig. 6 D, orange bars). Importantly, up-regulation of miR-451 combined with GSI treatment synergistically inhibited T-ALL cell growth (Fig. 6 E). Collectively, these results demonstrate that restoration of miR-451 expression could be considered as a novel therapeutic approach to reduce both the levels of MYC expression and T-ALL cell growth, especially in the context of GSI treatment.

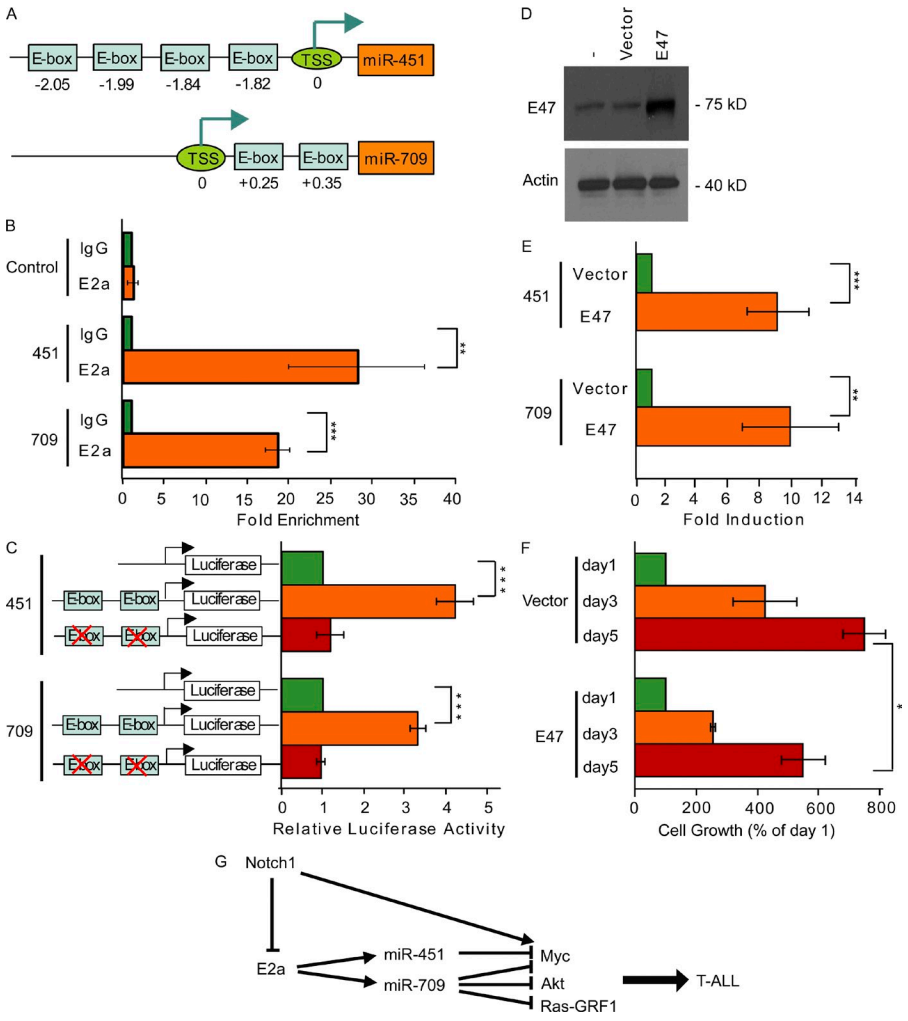

Figure 5. E2a transcriptionally activates miR-451 and miR-709. (A) Schematic presentation of miR-451 and miR-709 promoters. Positions (KB) of consensus E-box binding motifs (CANNTG) are indicated relative to the major transcription start site (TSS). (B) Quantitative ChIP analysis for normal mouse CD4$^+$CD8$^+$ thymocytes demonstrating E2a binding on miR-451 and miR-709 promoters. ChIP analysis was performed using an anti-E2A antibody or normal rabbit IgG (IgG negative control), followed by a quantitative PCR analysis using a negative control primer (Control) or specific primers for either miR-451 or miR-709 promoter. Fold enrichment was determined by a standard curve for the non-ChIP samples (input DNA). Data are presented as mean ± SD for triplicate experiments. **, $P < 0.01$; ***, $P < 0.001$. (C) Firefly luciferase constructs possessing miR-451 or miR-709 promoter with WT (orange) or mutated E-box motifs (red) was co-transfected with a renilla luciferase construct and an E47-expressing vector into NIH-3T3 cells. Firefly luciferase activity was normalized to renilla luciferase activity. Relative luciferase activity compared with the control vector without E-box motifs (green) was determined. Data are presented as mean ± SD for triplicate experiments. ***, $P < 0.001$. (D) Western Blot analysis of ectopically expressed, nondegradable mutant form of E47 (MSCV-IRES-GFP-MmE47) in ICN1-tranformed tumor cells (E47) compared with uninfected control (-) and MSCV-IRES-GFP retrovirus-infected ICN1-tranformed tumor cells (Vector). β-Actin, loading control. (E) miR-451 and miR-709 were measured by qRT-PCR in ICN1-trasnformed tumor cells expressing the nondegradable mutant form of E47 (E47) or control vector (Vector). Data are presented as mean ± SD for triplicate experiments. **, $P < 0.01$; ***, $P < 0.001$. (F) DsRed-ICN1 tumor cells were infected with MSCV-IRES-GFP-MmE47 (E47) or MSCV-IRES-GFP (Vector). GFP$^+$DsRed$^+$ cells were sorted and cultured, and cell growth was measured on days 1, 3, or 5. Data are presented as mean ± SD for triplicate experiments. *, $P < 0.05$. (G) Model for mechanism of Notch1-induced suppression of miR-451 and miR-709 in T-ALL. Increased Notch1 activity facilitates degradation of E2a, leading to transcriptional down-regulation of miR-451 and miR-709 that posttranscriptionally de-represses the T-ALL oncogenes Myc, Akt, and Ras-GRF1, which, in turn, promotes T-ALL. In addition, Notch1 has been shown to directly increase Myc transcription implying that Notch1 cooperates with reduced miR-451 and miR-709 to increase Myc expression.

DISCUSSION

We identified miR-451 and miR-709 as novel tumor suppressor miRNAs that normally repress the initiation and maintenance of mouse Notch1-driven leukemogenesis in vivo. Myc is essential for Notch1-induced T-ALL tumor formation in mice (Li et al., 2008) and has been shown to be an essential target of NOTCH1 in the maintenance of proliferation and viability in human and mouse T-ALL. Both miR-451 and miR-709 target Myc and Myc mRNA and protein levels are reduced by fivefold after transduction of tumor cells that results in near physiological levels of expression of miR-451 and miR-709. When both miRNAs were introduced together, Myc levels were reduced by ~10-fold, indicating that they act independently of other mechanisms to reduce Myc expression (Fig. 2 B).

It has been reported that miR-451 is underexpressed in cytogenetically normal acute myeloid leukemia patients (Whitman et al., 2010), and miR-451 functions as either a tumor suppressor (Gal et al., 2008; Nan et al., 2010) or an oncogene (Godlewski et al., 2010a,b) in human glioma cells. Here, we provide the first evidence showing that expression of both miR-451 and miR-709 in ICN1-expressing BM completely blocked the initiation of T-ALL in recipient mice (Fig. 4) leaving normal T cell development and the generation of nonmalignant ICN1-overexpressing cells intact, indicating that reduced expression of these tumor suppressor genes was required for transformation. Additionally, tumors developed with a significant delay when ICN1-overexpressing established tumor cells were transferred into nude mice after transduction with miR-451 or miR-709 to achieve levels similar to those in normal thymocytes (Fig. 3 and Fig. S2). These results clearly indicate the role of these miRNAs as tumor suppressors in T cell leukemogenesis. When tumor cells were transfected and the tumors that formed after a delay had selective loss of miRNA expression (Fig. 1 B), again supporting the selection for loss of these miRNAs in concert with ICN1 overexpression in T-ALL.

It is noted that copy number losses at these miRNA gene loci were not observed in mouse T-ALL, human primary T-ALL patient samples or cell lines by array-based CGH analysis (Li et al., 2008; Gutierrez et al., 2009; unpublished data). Thus, genetic deletion likely does not account for reduced expression of these miRNA gene loci in tumor cells. Our data demonstrate that ICN1 induction leads to E2a degradation and thus to reduced levels of miR-451 and miR-709, but we cannot exclude the possibility that epigenetic modifications can also participate in reducing expression of these miRNAs. Dicer-independent, but Argonaute2-dependent, biogenesis of miR-451 was recently reported (Cheloufi et al., 2010; Cifuentes et al., 2010).

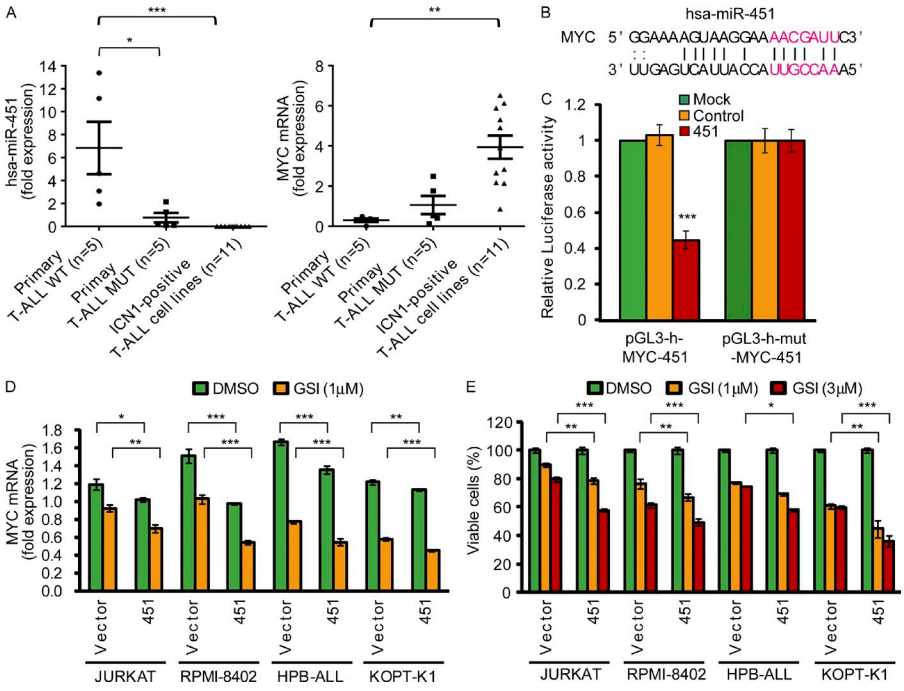

Figure 6. Activating *NOTCH1* mutations in human T-ALL demonstrate down-regulation of miR-451 and up-regulation of MYC. (A) human miR-451 and MYC RNA levels were assessed by quantitative RT-PCR in primary T-ALL samples clustered by WT or activating mutant (MUT) *NOTCH1* and in 11 ICN1-positive T-ALL cell lines. RNA expression levels of miR-451 or MYC were normalized by RNU1A or GAPDH, respectively, and fold expression is presented compared with the mean of normal thymocytes from two independent donor individuals. Significance was evaluated by the unpaired Student's *t* test: *, $P < 0.05$; **, $P < 0.01$; ***, $P < 0.001$. Data are shown as mean ± SEM for each group. (B) Computationally predicted miRNA–mRNA interactions between human miR-451 and the 3′UTR of human MYC (15–21, pink); miRNA binding sites were predicted by MIRANDA. (C) Firefly luciferase constructs possessing WT 3′UTRs or point mutant 3′UTRs (corresponding to seed region of miR-451) of human *MYC* was co-transfected with renilla luciferase constructs into NIH-3T3 cells alone (Mock), with a non-specific control (Control) or with a miR-451 (451). Firefly luciferase activity was normalized to renilla luciferase activity. Relative luciferase activity compared with Mock is shown. Data are presented as mean ± SD for triplicate experiments. ***, $P < 0.001$. (D) Four T-ALL cell lines were infected with the CMMP retrovirus encoding GFP and miR-451 (451) or no miRNA (Vector). After selection of GFP-positive cells by flow cytometry, the cells were treated without DMSO or with 1 μM MRK-003 γ-secretase inhibitor (GSI) for 3 d. Human MYC RNA levels were assessed by quantitative RT-PCR and normalized by GAPDH. Fold reduction is expressed as levels relative to levels in normal thymocytes. Error bars represent ± SD for triplicate experiments. *, $P < 0.05$; **, $P < 0.01$; ***, $P < 0.001$. (E) 4 T-ALL cell lines transduced with miR-451 (451) or no miRNA (Vector) were treated without DMSO or with 1 or 3 μM MRK-003 GSI for 5 d. Cell viability was measured by CellTiter-Glo assay and reported as percentage of DMSO-treated control. Error bars represent ± SD for triplicate experiments. *, $P < 0.05$; **, $P < 0.01$; ***, $P < 0.001$.

However, it is unlikely that this mechanism participates in T-ALL, because Argonaute2 expression was not reduced in human or mouse T-ALL (unpublished data) and pri-miR-451, premiR-451, and mature miR-451 were all reduced upon ICN1 induction (unpublished data) suggesting against posttranscriptional regulation of miR-451 levels.

Importantly, the human homologue of mouse miR-451 is robustly reduced in human T-ALLs that exhibit mutational activation of NOTCH1, with concomitant up-regulation of MYC expression similar to the results in mouse T-ALL. Humans do not contain miR-709, so miR-451 appears to subsume many of the MYC regulatory roles of both miR-451 and miR-709 in the mouse, which could be considered an advantage in terms of licensing miR-451 as a potential target for therapeutic intervention in T-ALL. miR-709 also down-regulates the AKT and RAS pathways in mouse T-ALL, and these pathways themselves are often directly mutated and activated in human T-ALL (Lübbert et al., 1990; Palomero et al., 2007; Gutierrez et al., 2009). We and others have previously demonstrated that genetic inactivation of *PTEN,* or mutational activation of *PI3K* or *AKT* genes occur in 47.7% of primary human T-ALL cases and that *RAS* gain-of-function mutations or *PTPN11* deletion occurs in 9.1 or 2.1% of cases, respectively (Lübbert et al., 1990; Palomero et al., 2007; Gutierrez et al., 2009). Thus, in humans, key components of these pathways are often directly altered by mutation to accomplish the same synergy required for transformation.

In conclusion, we demonstrate the first example of miRNA-mediated repression of tumor initiation in vivo. miR-451 is a suppressor of tumor initiation by acting to down-regulate MYC in both mouse and human T-ALL. Several miRNA gene knockout mice have been described (Rodriguez et al., 2007; Thai et al., 2007; Xiao et al., 2007) including a knockout mouse with targeted deletion of the DLEU2/miR-15a/miR-16-1 locus that predisposes the mice to chronic lymphocytic leukemia (Klein et al., 2010). However, the knockout locus also contains part of the DLEU1 gene and the DLEU2 gene and the DLEU2 gene product are implicated as suppressors of aggressive disease. In contrast, in the mouse model presented here, transcriptional activation driven by ICN1 cooperating with reduced posttranscriptional inhibition by miR-451 and miR-709 of T-ALL oncogenes is required for tumor initiation and maintenance, suggesting that these miRNAs represent important biomarkers and possible candidates for therapeutic reconstitution.

MATERIALS AND METHODS

miRNA microarray analysis

Total RNA for miRNA expression profiling was extracted using TRIzol Reagent (Invitrogen) from the three groups of the mouse cells: control $CD4^+8^+$ thymocytes, nonmalignant ICN1 overexpressing $CD4^+8^+$ cells, and T-ALL tumor $CD4^+8^+$ cells. miRNA microarray analysis was performed using the mercury Hy3/Hy5 labeling kit and the mercury LNA array (version 8.1; both from Exiqon A/S). The microarray data have been deposited in the GEO database under accession no. GSE27418.

Mice

BALB/c WT and BALB/c Nu/Nu mice were purchased from Taconic. All mice were kept in specific pathogen–free animal facilities at the Dana-Farber Cancer Institute (Boston, MA). All animal procedures were performed in compliance with the guidelines of the Dana-Farber Cancer Institute Animal Resources Facility, which operates under regulatory requirement of the U.S. Department of Agriculture and Association for Assessment and Accreditation of Laboratory Animal Care. Experimental protocols were approved by the Animal Care and Use Committee of the Dana-Farber Cancer Institute.

miRNA precursor cloning and construction of retroviral vectors

miR-451 and miR-709 precursors were PCR-amplified from mouse genomic DNA. Amplified fragments were subcloned into the pEGP-miR cloning vector (Cell Biolabs, Inc.) between BamH1 and NheI sites, and then the fragment of EF-1 Promoter/human β-globin intron containing the miRNA precursor was subcloned into a bicistronic retroviral vector MSCV-IRES-GFP between EcoRI and SnaBI. To preserve the putative hairpin structure and endogenous processing, miRNA stem loop sequence was flanked by its native intron sequence. The sequences of PCR primers for miR-451 precursor were (forward) 5′-TCGAGGATCCCTGGGTACCCCACCTCCAGAGCCT-3′ and (reverse) 5′-TCGAGCTAGCAAAATGTACCCTTTCCCCCAACCCCATT-3′. The sequences of PCR primers for miR-709 precursor were (forward) 5′-TCGAGCTAGCAAGGAGAGAGAAAACGGACTCCTCTAGGTT-3′ and (reverse) 5′-TCGAGCTAGCAAGGAGAGAGAAAACGGACTCCTCTAGGTT-3′. The miR-451+miR-709 fragment was generated by overlapping PCR. Another bicistronic retroviral vector, CMMP-IRES-EGFP, was used to construct the miRNA retroviral vector. The PCR-amplified fragment was cloned into the retroviral vector under control of the cytomegalovirus promoter. The miRNA transgene expression was confirmed by real-time PCR. The sequences of PCR primers for the miR-451 precursor were (forward) 5′-TCCTCGAGCTGGGTACCCCACCTCCAGAGCCT-3′ and (reverse) 5′-TAGGATCCAAAATGTACCCTTTCCCCCAACCCCATT-3′. The sequences of PCR primers for the miR-709 precursor were (forward) 5′-TCCTCGAGAGGGTAGCCTTGAACTCAGAGATTTGCC-3′ and (reverse) 5′-TAGGATCCAAGGAGAGAGAAAACGGACTCCTCTAGGTT-3′.

Retrovirus production and BM transplantation

Retroviral supernatants were produced by transfection of 293T cells with retroviral constructs and appropriate packaging vectors, as previously described (Li et al., 2008). Retroviral infection and BM reconstitution were performed as follows: Lin^- (CD3ε, TCR-β, NK1.1, DX5, CD19, Ter-119, Mac-1, and Gr-1) BM cells were sorted from BALB/c mice and cultured with Flt3L, IL-6, IL-7, and Scf (all from R&D Systems). On days 2 and 4 after sorting, cells were subjected to retroviral infection with MSCV-ICN1-IRES-DsRed retrovirus and CMMP-IRES-EGFP, or CMMP-miR-451+709-IRES-EGFP retrovirus by centrifugation at 2,300 rpm for 1.5 h at room temperature. GFP^+DsRed^+ cells were collected by FACS sorting and injected intravenously into sublethally irradiated 4–6-wk-old syngeneic BALB/c recipient mice.

Ectopic expression of miR-451 and miR-709

$DsRed^+$ICN1-overexpressing T-ALL cells were isolated from ICN1-dependent tumor cells in BALB/c mice after BM transplantation. Tumor cells were maintained in RPMI-1640 medium supplemented with 10% fetal bovine serum, penicillin G, and streptomycin in a humidified atmosphere containing 5% CO_2 at 37°C. $DsRed^+$ tumor cells were infected with a GFP-expressing retrovirus (MSCV-IRES-EGFP) also expressing nothing (empty vector control) or expressing miR-451 (MSCV-miR-451-IRES-EGFP), miR-709 (MSCV-miR-709-IRES-EGFP), or miR-451 and miR-709 in tandem (MSCV-miR-451+709-IRES-EGFP). After 48 h, GFP^+/Ds-red^+ cells were sorted, collected, and injected into nude (Nu/Nu; Taconic) mice.

Dual luciferase assays

miRNA target validation. 3′UTR segments of mouse Myc, Akt or Ras-GRF1 or 3′UTR segment of human MYC were amplified by PCR from mouse genomic DNA or human genomic DNA using the following primers: 5′-CATCTAGAACTGACCTAACTCGAGGA-3′ (Myc-3UTR-F)

and 5′-GCTCTAGATTATTTACATTTCAAGGC-3′ (Myc-3UTR-R); 5′-CATCTAGAAGAGGTCACAGCTGCTTCA-3′ (Akt-3UTR-F) and 5′-GCTCTAGACAAGCTTGAAAAGCAATTT-3′ (Akt-3UTR-R); 5′-CATCTAGAGGCTGTTCTCCCCACCCACTGGCA-3′ (Ras-GRF1-3UTR-F) and 5′-GCTCTAGACGTCACAGAAAGGGAGGCAGAGTCTGAGAGTGCA-3′ (Ras-GRF1-3UTR-R), 5′-CATCTAGAGGAAAAGTAAGGAAAACGATTCCTTCT-3′ (human-MYC-3UTR-F) and 5′-GCTCTAGATATTAAAGTTATTTACATTTAATGGCA-3′ (human-MYC-3UTR-R). The segments were then cloned into a firefly luciferase reporter vector pGL3 control vector (Promega) using the XbaI site immediately downstream from the stop codon of luciferase, giving rise to the pGL3-Myc, pGL3-Akt, pGL3-Ras-GRF1, pGL3-h-MYC WT plasmid, respectively. The WT insert was used to generate the insert with point mutation from the site of perfect complementarity by using the following primers: 5′-CATCTAGAACTGACCTAACTCGAGGAGGAGCTGGAATCTCTCGTGAGAGTAAGGAGTCGCCGGCCTTCT-3′ (Myc-mut-451-F) and 5′-GCTCTAGATTATTTACATTTCAAGGC-3′ (Myc-mut-451-R); 5′-GCCATAATTTTAAACCGGGGAAACTTAAATAGTA-3′ (Myc-mut-709-F) and 5′-TACTATTTAAGTTTCCCCGGTTTAAAATTATGGC-3′ (Myc-mut-709-R); 5′-TACCCTGGGAGCGCGCAGTATACGTGAGCCCTTCTC-3′ (Akt-mut-F) and 5′-AGAAGGGCTCACGTATACTGCGCGCTCCCAGGGTA-3′ (Akt-mut-R); 5′-CATCTAGAGGCTGTTCTCCCCACCCACTGGCA-3′ (Ras-GRF1-mut-F) and 5′-CATCTAGAGGCTGTTCTCCCCACCCACTGGCACCGCAGCGTAACGCCAGGCAGTATCCAGGCAGTATTG-3′ (Ras-GRF1-mut-R); 5′-CATCTAGAGGAAAAGTAAGGAATCGCCGGCCTTCTAACA-3′ (human-MYC-mut-F) and 5′-GCTCTAGATATTAAAGTTATTTACATTTAATGGCA-3′ (human-MYC-mut-R). The mutant insert was cloned into pGL3-control vector using the same cloning site as WT, named pGL3-Myc-mut-451, pGL3-Myc-mut-709, pGL3-Akt-mut, pGL3-Ras-GRF1-mut, pGL3-h-MYC-mut-451 plasmid, respectively. WT and mutant inserts were confirmed by DNA sequencing. NIH3T3 cells were transfected in 12-well plates using Lipofectamine2000 (Invitrogen) according to the manufacturer's protocol. In brief, 30 nM miRNA (nonspecific mimic control, miR-451 mimic, or miR-709) was co-transfected with 0.6 μg of the firefly luciferase construct containing a WT or a mutated 3′UTR and 0.1 μg of the control reporter vector pRL-TK containing renilla luciferase (Promega). The sequences of miR-451 and miR-709 binding sites in WT 3′UTRs or point mutant 3′UTRs (corresponding to the seed region of miR-451 and miR-709) cloned into luciferase reporter constructs are as follows: mmu-miR-451-c-Myc: WT 5′-CGTGAGAGTAAGGAGAACGGTTC-3′; mutant 5′-CGTGAGAGTAAGGAGTCGCCGGC-3′. Mmu-miR-709-c-Myc: WT 5′-CAGCCATAATTTTAACTGCCTCA-3′, mutant 5′-CAGCCATAATTTTAAACCGGGA-3′. mmu-miR-709-Akt: WT 5′-GTACCCTGGGAGCGCCTGCCTCA-3′, mutant 5′-GTACCCTGGGAGCGCGCAGTATA-3′. mmu-miR-709-Ras-GRF1: WT 5′-CTGCACTCTCAGCTCTGCCTCC-3′, mutant 5′-CTGCACTCTCAGACTGCAGTATC-3′. hsa-miR-451-c-Myc: WT 5′-GGAAAAGTAAGGAAAACGATTC-3′, mutant 5′-GGAAAAGTAAGGAATCGCCGGC-3′. Firefly and renilla luciferase activities were measured consecutively using the dual luciferase assay (Promega) 24h after transfection. Firefly luciferase activity was normalized to renilla luciferase activity.

E2A Transcriptional activation. A fragment containing two E-box motifs in the promoter region of mmu-miR-451 or mmu-miR-709 was PCR amplified from mouse genomic DNA by using the following primers: 5′-AATGGTACCTAGGCTGCTACCCTGATAGT-3′ and 5′-ATTGCTAGCTTTCCTCAAATGTAAGATGGA-3′ for miR-451; 5′-ATGGTACCAATCTTCATTCGGGTGGCCATGAGTT-3′ and 5′-ATGCTAGCAACACTAGCACCTGGGGCATTCTGT-3′ for miR-709. The PCR products were cloned into the KpnI–NheI restriction endonuclease cleavage sites of the pGL4.10[luc2] luciferase reporter vector (Promega) to generate luciferase reporter construct pGL4.10-miR-451-WT for mmu-miR-451 and pGL4.10-miR-709-WT for mmu-miR-709, respectively. The WT insert was used to generate the insert with deletion of E-box motif by PCR-mediated site-directed mutagenesis/deletion using the following primer pairs: 5′-AATGGTACCTAGGCTGCTACCCTGATAGT-3′ and 5′-CCAGCACACTGTGCCTCTTGTCTCTCCTTCT-3′, 5′-AGAAGGAGAGACAAGAGGCACAGTGTGCTGG-3′ and 5′-ATGCTAGCTAAGATGGAGCTCTTGGTGTCCT-3′, 5′-AATGGTACCTAGGCTGCTACCCTGATAGT-3′ and 5′-ATGCTAGCTAAGATGGAGCTCTTGGTGTCCT-3′ for miR-451 E-box-deletion mutant reporter construct (pGL4.10-miR-451-dE-box) and 5′-ATGGTACCAATCTTCATTCGGGTGGCCATGAGTT-3′ and 5′-TGCTGCGGCAGGAGTGGGGGCAGCAT-3′, 5′-ATGCTGCCCCCACTCCTGCCGCAGCA-3′ and 5′-AATGCTAGCCATTCTGTGGATCCTGAC-3′, and 5′-ATGGTACCAATCTTCATTCGGGTGGCCATGAGTT-3′ and 5′-AATGCTAGCCATTCTGTGGATCCTGAC-3′ for miR-709 E-box-deletion mutant reporter construct (pGL4.10-miR-709-dE-box). NIH3T3 cells were transfected in 12-well plates using Lipofectamine 2000 (Invitrogen) according to the manufacturer's protocol. In brief, 2 μg of E47-pcDNA3 (Nie et al., 2003; provided by X.-H. Sun, Oklahoma Medical Research Foundation) was co-transfected with 1 μg of the firefly luciferase construct containing a WT or a deleted E-box motif and 0.1 μg of the control reporter vector pRL-TK containing Renilla luciferase (Promega). Firefly and Renilla luciferase activities were measured consecutively using the dual luciferase assay (Promega) 24 h after transfection according to the manufacturer's instructions. Firefly luciferase activity was normalized to Renilla luciferase activity.

Transfection of miRNA mimics

ICN1-overexpressing T-ALL cells were isolated and transfected with mmu-miR-451 mimic, mmu-miR-709 mimic or control miRNA mimic (Thermo Fisher Scientific) with Cy3-labeled oligonucleotides (1:3 relative amount of miRNA mimics) at a final concentration of 100 nM by Lipofectamine 2000 (Invitrogen).

Quantitative analysis of miRNA expression

For analysis of miRNA expression in normal thymocytes, total RNA was extracted using the TRIzol reagent (Invitrogen). TaqMan miRNA assays (Applied Biosystems) were used to measure miR-451 and miR-709 expression in various T cell subsets and transduced ICN1 tumor cells. U6 snRNA was used as an internal control to normalize expression. Specific stem-loop miRNA primers for reverse transcription and TaqMan probes for miR451, miR-709, and U6 snRNA were purchased from ABI. For analysis of miRNA expression in ICN1-transformed tumor cells, total RNA was extracted using TRIzol reagent (Invitrogen) and was reverse transcribed to cDNA using miScript Reverse Transcription kit (QIAGEN). To quantify the miRNA levels, the ABI7300 real time PCR system (Applied Biosystems) was used in conjunction with miScript SYBR Green PCR kit (QIAGEN) for mmu-miR-451, mmu-miR-709, mouse RNU6B, hsa-miR-451, and human RNU1A. RNU6B or RNU1A was used as an endogenous control to normalize expression. Specific primers for mmu-miR-451, mmu-miR-709, mouse RNU6B, hsa-miR-451, and human RNU1A were purchased from QIAGEN.

Quantitative RT-PCR analysis of protein-coding genes

cDNA was prepared by the oligo-dT primer method using the Superscript II Reverse Transcription kit (Invitrogen). Quantitative RT-PCR was performed using an ABI7300 machine (Applied Biosystems). Mouse Myc, Akt, and Ras-GRF1 mRNA were determined relative to GAPDH expression using the TaqMan Gene Expression Assay (Applied Biosystems). Human MYC mRNAs was determined relative to GAPDH expression using SYBR Green (Applied Biosystems) and the following primers: MYC forward, 5′-CTCTCCGTCCTCGGATTCT-3′, MYC reverse, 5′-CAACATCGATTTCTTCCTCATC-3′, GAPDH forward, 5′-CTCCTCTGACTTCAACAGCGACAC-3′, GAPDH reverse, 5′-TGCTGTAGCCAAATTCGTTGTCAT-3′.

ChIP assay

ChIP analysis was performed on mouse normal thymocytes according to the manufacturer's protocol (ChIP-IT Express protocol; Active Motif). In brief, cells were cross-linked with 1% formaldehyde for 5 min at room temperature,

and the reaction was stopped by the addition of 1x Glycine. Cells were lysed in ChIP lysis buffer, and then sonicated to shear chromatin into 200–1,000-bp fragments. Chromatin was immunoprecipitated with anti-E2A polyclonal antibody (Santa Cruz Biotechnology, Inc.) or with normal rabbit IgG antibody (Santa Cruz Biotechnology, Inc.) incubated with protein G magnetic beads. After immunoprecipitation, cross-linking was reversed, the proteins were removed by treatment with Proteinase K, and DNA was recovered. DNA was purified by phenol/chloroform extraction and ethanol precipitation. PCR was performed for miRNA promoter regions encompassing putative E2A binding motifs. PCR products were quantified by using SYBR green dye on an ABI 7300 real-time PCR machine. Fold enrichment was determined by performing a standard curve of input DNA. Primers used for the amplicon containing the two distal E box binding sites on the mmu-miR-451 enhancer were: forward, 5′-TAATGAGGCAAAGAGAAGGAGAGAC-3′; reverse, 5′-ACAGCTCACTACATCCAGCTCTGTGA-3′. Primers used for the amplicon containing the two E-box binding sites on the mmu-miR-709 enhancer were: forward, 5′-AGCAGCAGCCGCTCCATTACGA-3′; reverse, 5′-AACACTAGCACCTGGGGCATTCT-3′. Control primers for the nonbinding site were: forward, 5′-AAGGGTGGAGCCAAAGGGTCA-3′; reverse, 5′-TGGTGCAGGATGCATTGCTGAC-3′.

Western blotting

T-ALL cells infected with either retroviral vector control, or retroviruses expressing the miR-451 mimic, the miR-709 mimic, or the miR-451 and miR-709 mimics in tandem were lysed in radioimmunoprecipitation assay buffer supplemented with Protease Inhibitor Cocktail (Sigma-Aldrich). Lysates (12 μg) were separated on 4–20% SDS-PAGE and transferred onto PVDF membrane (Millipore). Nonspecific binding was blocked by incubation in blocking buffer (5% nonfat milk in TBST), followed by incubation with the primary antibodies against Myc (Abcam), Akt, Ras-GRF1, E47 (BD), or β-actin (Sigma-Aldrich) and the appropriate horseradish peroxidase–conjugated secondary antibodies diluted in blocking buffer. Immunoreactive proteins were detected using enhanced chemiluminescence reagents (GE Healthcare).

Cell viability assays

DsRed-ICN1 tumor cells were transduced by retroviral infection of MSCV-IRES-GFP-MmE47 construct or MSCV-IRES-GFP empty vector as control. $GFP^+/DsRed^+$ cells were sorted and seeded into 96-well plates at a density of 4×10^3 cells/well and incubated for 5 d. Cell viability assay was determined on days 1, 3, and 5 of incubation by CellTiter-Glo luminescent reagent (Promega).

Tumor formation assays

4–5-wk-old Nude mice (Nu/Nu, Taconic) were adoptively transferred with T-ALL cells infected with retroviruses expressing nothing (vector control) or expressing miR-451, miR-709, or both miR-451 and miR-709 in tandem. Approximately 3×10^5 cells were intraperitoneally injected into Nu/Nu mice and tumor formation was monitored.

Histopathology

Tissue samples were fixed in 10% formalin solution (Sigma-Aldrich). Hematoxylin and eosin staining of various tissues, May Grunwald-Giemsa staining of blood smear and immunohistochemistry analysis using anti-CD4, -CD8, and -Ki67 antibodies were conducted in the Hematopathology Core facility of Dana-Farber/Harvard Cancer Center Research Pathology Core using standard staining procedures.

Primary human T-ALL samples and cell lines

T-ALL diagnostic specimens were collected with informed consent and Institutional Review Board approval from 10 patients treated in Dana-Farber Cancer Institute study 00–001 (Clinicaltrials.gov identifier: NCT00165178. http://clinicaltrials.gov/ct2/show/NCT00165178?term=NCT00165178&rank=1.), as previously described (Gutierrez et al., 2009). All samples were purified to >90% lymphoblasts by centrifugation with Ficoll-Hypaque (Roche). The detailed information for each primary sample is described in Table S1. Thymocytes were obtained with informed consent and Institutional Review Board approval from normal thymic tissue removed at the time of cardiac surgery at the Children's Hospital Boston (Boston, MA). 11 human T-ALL cell lines (DU528, JURKAT, PEER, DND-41, HPB-ALL, KOPT-K1, MOLT-4, PF-382, SUP-T7, CCRF-CEM, and RPMI-8402) were used in this study. Sequencing of exons 28, 29, and 34 of the human *NOTCH1* gene, and exons 9 and 10 of the human *FBXW7* gene, was performed on human T-ALL primary samples at Beckman Coulter. RNA was extracted using TRIzol reagent according to the manufacturer's instructions (Invitrogen).

Overexpression of miR-451 and GSI treatment of human T-ALL cell lines

Retroviruses encoding EGFP and miR-451 or no miRNA were produced by 293T cells co-transfected with the CMMP retroviral construct, a packaging plasmid gag-pol, and an envelope plasmid VSV-G. 4 human T-ALL cell lines (JURKAT, RPMI-8402, HPB-ALL, and KOPT-K1) were infected with retroviruses in the presence of polybrene by centrifugation at 2,500 rpm for 1.5 h. EGFP-positive cells were sorted by flow cytometry. For RNA analysis, the cells were treated with DMSO or MRK-003 GSI (provided by Merck Research Laboratory) for 3 d. For cell viability analysis, the cells were treated with DMSO or GSI for 5 d in 96-well plates and cell viability was measured by CellTiter-Glo (Promega).

Online supplemental material

Fig. S1 shows dynamic regulation of miR-451 and miR-709 expressions during normal thymocyte development and correlation of miR-451 expression with GFP expression in cells infected with the GFP-miR-451–expressing vector. Fig. S2 demonstrates that reconstitution of miR-451 and miR-709 by transfection represses T-ALL tumor formation in vivo. Fig. S3 indicates that coordinate expression of miR-451 and miR-709 blocks ICN1-induced tumor initiation in vivo. Fig. S4 shows that expression of miR-451 and miR-709 in BM cells does not block the generation of extrathymic, nontumorigenic, $CD4^+CD8^+$ cells during the early stages after BM transplantation. Fig. S5 shows overexpression of miR-451 in human T-ALL cell lines. Table S1 shows the genetic status of *NOTCH1* and *FBXW7* genes and expressions of cell surface markers in primary T-ALL and cell lines. Online supplemental material is available at http://www.jem.org/cgi/content/full/jem.20102384/DC1.

We would like to gratefully acknowledge the patients with T-ALL and their families. We thank Drs. Lewis B. Silverman and Stephen E. Sallan, as well as members of the Dana-Farber Cancer Institute Acute Lymphoblastic Leukemia Consortium member institutions, for the samples analyzed in this study. We wish to thank Merck Research Laboratories for generously providing GSI MRK-003. We wish to thank Drs. Shuqiang Li for assistance with miRNA expression profiling, Taras Kreslavskiy for sorting DN-SP thymocytes, Alexander Marson and Dimitrios Iliopoulos for assistance with miRNAs Promoter/Enhancer analysis, Etienne Gagnon for assistance with figure production, Alejandro Gutierrez for annotating the *NOTCH1* and *FBXW7* genes, and Howell Moffat for critically reading this manuscript.

This work was funded by National Cancer Institute grants 5P01CA109901 (A.T. Look and H. von Boehmer) and 5P01CA68484 (A.T. Look); by a Jose Carreras International Leukemia Foundation grant (C.D. Novina); by the Claudia Adams Barr grant (X. Li); and by the Children's Leukemia Research Association (T. Sanda).

The authors have no conflicting financial interests.

Submitted: 15 November 2010
Accepted: 25 February 2011

REFERENCES

Armstrong, S.A., and A.T. Look. 2005. Molecular genetics of acute lymphoblastic leukemia. *J. Clin. Oncol.* 23:6306–6315. doi:10.1200/JCO.2005.05.047

Bain, G., E.C. Maandag, D.J. Izon, D. Amsen, A.M. Kruisbeek, B.C. Weintraub, I. Krop, M.S. Schlissel, A.J. Feeney, M. van Roon, et al. 1994. E2A proteins are required for proper B cell development and initiation of immunoglobulin gene rearrangements. *Cell.* 79:885–892. doi:10.1016/0092-8674(94)90077-9

Bain, G., I. Engel, E.C. Robanus Maandag, H.P. te Riele, J.R. Voland, L.L. Sharp, J. Chun, B. Huey, D. Pinkel, and C. Murre. 1997. E2A deficiency leads to abnormalities in alphabeta T-cell development and to rapid development of T-cell lymphomas. *Mol. Cell. Biol.* 17:4782–4791.

Bonci, D., V. Coppola, M. Musumeci, A. Addario, R. Giuffrida, L. Memeo, L. D'Urso, A. Pagliuca, M. Biffoni, C. Labbaye, et al. 2008. The miR-15a-miR-16-1 cluster controls prostate cancer by targeting multiple oncogenic activities. *Nat. Med.* 14:1271–1277. doi:10.1038/nm.1880

Calin, G.A., M. Ferracin, A. Cimmino, G. Di Leva, M. Shimizu, S.E. Wojcik, M.V. Iorio, R. Visone, N.I. Sever, M. Fabbri, et al. 2005. A MicroRNA signature associated with prognosis and progression in chronic lymphocytic leukemia. *N. Engl. J. Med.* 353:1793–1801. doi:10.1056/NEJMoa050995

Cheloufi, S., C.O. Dos Santos, M.M. Chong, and G.J. Hannon. 2010. A dicer-independent miRNA biogenesis pathway that requires Ago catalysis. *Nature*. 465:584–589. doi:10.1038/nature09092

Cifuentes, D., H. Xue, D.W. Taylor, H. Patnode, Y. Mishima, S. Cheloufi, E. Ma, S. Mane, G.J. Hannon, N.D. Lawson, et al. 2010. A novel miRNA processing pathway independent of Dicer requires Argonaute2 catalytic activity. *Science*. 328:1694–1698. doi:10.1126/science.1190809

Cimmino, A., G.A. Calin, M. Fabbri, M.V. Iorio, M. Ferracin, M. Shimizu, S.E. Wojcik, R.I. Aqeilan, S. Zupo, M. Dono, et al. 2005. miR-15 and miR-16 induce apoptosis by targeting BCL2. *Proc. Natl. Acad. Sci. USA*. 102:13944–13949. doi:10.1073/pnas.0506654102

Ellisen, L.W., J. Bird, D.C. West, A.L. Soreng, T.C. Reynolds, S.D. Smith, and J. Sklar. 1991. TAN-1, the human homolog of the *Drosophila* notch gene, is broken by chromosomal translocations in T lymphoblastic neoplasms. *Cell*. 66:649–661. doi:10.1016/0092-8674(91)90111-B

Gal, H., G. Pandi, A.A. Kanner, Z. Ram, G. Lithwick-Yanai, N. Amariglio, G. Rechavi, and D. Givol. 2008. MIR-451 and Imatinib mesylate inhibit tumor growth of Glioblastoma stem cells. *Biochem. Biophys. Res. Commun.* 376:86–90. doi:10.1016/j.bbrc.2008.08.107

Girard, L., Z. Hanna, N. Beaulieu, C.D. Hoemann, C. Simard, C.A. Kozak, and P. Jolicoeur. 1996. Frequent provirus insertional mutagenesis of Notch1 in thymomas of MMTVD/myc transgenic mice suggests a collaboration of c-myc and Notch1 for oncogenesis. *Genes Dev.* 10:1930–1944. doi:10.1101/gad.10.15.1930

Godlewski, J., A. Bronisz, M.O. Nowicki, E.A. Chiocca, and S. Lawler. 2010a. microRNA-451: a conditional switch controlling glioma cell proliferation and migration. *Cell Cycle*. 9:2742–2748. doi:10.4161/cc.9.14.12248

Godlewski, J., M.O. Nowicki, A. Bronisz, G. Nuovo, J. Palatini, M. De Lay, J. Van Brocklyn, M.C. Ostrowski, E.A. Chiocca, and S.E. Lawler. 2010b. MicroRNA-451 regulates LKB1/AMPK signaling and allows adaptation to metabolic stress in glioma cells. *Mol. Cell.* 37:620–632. doi:10.1016/j.molcel.2010.02.018

Gutierrez, A., T. Sanda, R. Grebliunaite, A. Carracedo, L. Salmena, Y. Ahn, S. Dahlberg, D. Neuberg, L.A. Moreau, S.S. Winter, et al. 2009. High frequency of PTEN, PI3K, and AKT abnormalities in T-cell acute lymphoblastic leukemia. *Blood*. 114:647–650. doi:10.1182/blood-2009-02-206722

He, L., J.M. Thomson, M.T. Hemann, E. Hernando-Monge, D. Mu, S. Goodson, S. Powers, C. Cordon-Cardo, S.W. Lowe, G.J. Hannon, and S.M. Hammond. 2005. A microRNA polycistron as a potential human oncogene. *Nature*. 435:828–833. doi:10.1038/nature03552

Ikawa, T., H. Kawamoto, A.W. Goldrath, and C. Murre. 2006. E proteins and Notch signaling cooperate to promote T cell lineage specification and commitment. *J. Exp. Med.* 203:1329–1342. doi:10.1084/jem.20060268

John, B., A.J. Enright, A. Aravin, T. Tuschl, C. Sander, and D.S. Marks. 2004. Human microRNA targets. *PLoS Biol.* 2:e363. doi:10.1371/journal.pbio.0020363

Johnson, S.M., H. Grosshans, J. Shingara, M. Byrom, R. Jarvis, A. Cheng, E. Labourier, K.L. Reinert, D. Brown, and F.J. Slack. 2005. RAS is regulated by the let-7 microRNA family. *Cell*. 120:635–647. doi:10.1016/j.cell.2005.01.014

Klein, U., M. Lia, M. Crespo, R. Siegel, Q. Shen, T. Mo, A. Ambesi-Impiombato, A. Califano, A. Migliazza, G. Bhagat, and R. Dalla-Favera. 2010. The DLEU2/miR-15a/16-1 cluster controls B cell proliferation and its deletion leads to chronic lymphocytic leukemia. *Cancer Cell*. 17:28–40. doi:10.1016/j.ccr.2009.11.019

Lee, Y.S., and A. Dutta. 2007. The tumor suppressor microRNA let-7 represses the HMGA2 oncogene. *Genes Dev.* 21:1025–1030. doi:10.1101/gad.1540407

Lewis, B.P., I.H. Shih, M.W. Jones-Rhoades, D.P. Bartel, and C.B. Burge. 2003. Prediction of mammalian microRNA targets. *Cell*. 115:787–798. doi:10.1016/S0092-8674(03)01018-3

Li, Q.J., J. Chau, P.J. Ebert, G. Sylvester, H. Min, G. Liu, R. Braich, M. Manoharan, J. Soutschek, P. Skare, et al. 2007. miR-181a is an intrinsic modulator of T cell sensitivity and selection. *Cell*. 129:147–161. doi:10.1016/j.cell.2007.03.008

Li, X., F. Gounari, A. Protopopov, K. Khazaie, and H. von Boehmer. 2008. Oncogenesis of T-ALL and nonmalignant consequences of overexpressing intracellular NOTCH1. *J. Exp. Med.* 205:2851–2861. doi:10.1084/jem.20081561

Lu, J., G. Getz, E.A. Miska, E. Alvarez-Saavedra, J. Lamb, D. Peck, A. Sweet-Cordero, B.L. Ebert, R.H. Mak, A.A. Ferrando, et al. 2005. MicroRNA expression profiles classify human cancers. *Nature*. 435:834–838. doi:10.1038/nature03702

Lübbert, M., J. Mirro Jr., C.W. Miller, J. Kahan, G. Isaac, G. Kitchingman, R. Mertelsmann, F. Herrmann, F. McCormick, and H.P. Koeffler. 1990. N-ras gene point mutations in childhood acute lymphocytic leukemia correlate with a poor prognosis. *Blood*. 75:1163–1169.

Mavrakis, K.J., A.L. Wolfe, E. Oricchio, T. Palomero, K. de Keersmaecker, K. McJunkin, J. Zuber, T. James, A.A. Khan, C.S. Leslie, et al. 2010. Genome-wide RNA-mediated interference screen identifies miR-19 targets in Notch-induced T-cell acute lymphoblastic leukaemia. *Nat. Cell Biol.* 12:372–379. doi:10.1038/ncb2037

Nan, Y., L. Han, A. Zhang, G. Wang, Z. Jia, Y. Yang, X. Yue, P. Pu, Y. Zhong, and C. Kang. 2010. MiRNA-451 plays a role as tumor suppressor in human glioma cells. *Brain Res.* 1359:14–21. doi:10.1016/j.brainres.2010.08.074

Nie, L., M. Xu, A. Vladimirova, and X.H. Sun. 2003. Notch-induced E2A ubiquitination and degradation are controlled by MAP kinase activities. *EMBO J.* 22:5780–5792. doi:10.1093/emboj/cdg567

O'Donnell, K.A., E.A. Wentzel, K.I. Zeller, C.V. Dang, and J.T. Mendell. 2005. c-Myc-regulated microRNAs modulate E2F1 expression. *Nature*. 435:839–843. doi:10.1038/nature03677

O'Neil, J., J. Grim, P. Strack, S. Rao, D. Tibbitts, C. Winter, J. Hardwick, M. Welcker, J.P. Meijerink, R. Pieters, et al. 2007. FBW7 mutations in leukemic cells mediate NOTCH pathway activation and resistance to gamma-secretase inhibitors. *J. Exp. Med.* 204:1813–1824. doi:10.1084/jem.20070876

Ortholan, C., M.P. Puissegur, M. Ilie, P. Barbry, B. Mari, and P. Hofman. 2009. MicroRNAs and lung cancer: new oncogenes and tumor suppressors, new prognostic factors and potential therapeutic targets. *Curr. Med. Chem.* 16:1047–1061. doi:10.2174/092986709787581833

Paganin, M., and A. Ferrando. 2011. Molecular pathogenesis and targeted therapies for NOTCH1-induced T-cell acute lymphoblastic leukemia. *Blood Rev.* 25:83–90.

Palomero, T., W.K. Lim, D.T. Odom, M.L. Sulis, P.J. Real, A. Margolin, K.C. Barnes, J. O'Neil, D. Neuberg, A.P. Weng, et al. 2006. NOTCH1 directly regulates c-MYC and activates a feed-forward-loop transcriptional network promoting leukemic cell growth. *Proc. Natl. Acad. Sci. USA*. 103:18261–18266. doi:10.1073/pnas.0606108103

Palomero, T., M.L. Sulis, M. Cortina, P.J. Real, K. Barnes, M. Ciofani, E. Caparros, J. Buteau, K. Brown, S.L. Perkins, et al. 2007. Mutational loss of PTEN induces resistance to NOTCH1 inhibition in T-cell leukemia. *Nat. Med.* 13:1203–1210. doi:10.1038/nm1636

Pear, W.S., J.C. Aster, M.L. Scott, R.P. Hasserjian, B. Soffer, J. Sklar, and D. Baltimore. 1996. Exclusive development of T cell neoplasms in mice transplanted with bone marrow expressing activated Notch alleles. *J. Exp. Med.* 183:2283–2291. doi:10.1084/jem.183.5.2283

Pece, S., M. Serresi, E. Santolini, M. Capra, E. Hulleman, V. Galimberti, S. Zurrida, P. Maisonneuve, G. Viale, and P.P. Di Fiore. 2004. Loss of negative regulation by Numb over Notch is relevant to human breast carcinogenesis. *J. Cell Biol.* 167:215–221. doi:10.1083/jcb.200406140

Rodriguez, A., E. Vigorito, S. Clare, M.V. Warren, P. Couttet, D.R. Soond, S. van Dongen, R.J. Grocock, P.P. Das, E.A. Miska, et al. 2007. Requirement of bic/microRNA-155 for normal immune function. *Science*. 316:608–611. doi:10.1126/science.1139253

Sade, H., S. Krishna, and A. Sarin. 2004. The anti-apoptotic effect of Notch-1 requires p56lck-dependent, Akt/PKB-mediated signaling in T cells. *J. Biol. Chem.* 279:2937–2944. doi:10.1074/jbc.M309924200

Sanda, T., X. Li, A. Gutierrez, Y. Ahn, D.S. Neuberg, J. O'Neil, P.R. Strack, C.G. Winter, S.S. Winter, R.S. Larson, et al. 2010. Interconnecting molecular pathways in the pathogenesis and drug sensitivity of T-cell acute lymphoblastic leukemia. *Blood.* 115:1735–1745. doi:10.1182/blood-2009-07-235143

Sharma, V.M., J.A. Calvo, K.M. Draheim, L.A. Cunningham, N. Hermance, L. Beverly, V. Krishnamoorthy, M. Bhasin, A.J. Capobianco, and M.A. Kelliher. 2006. Notch1 contributes to mouse T-cell leukemia by directly inducing the expression of c-myc. *Mol. Cell. Biol.* 26:8022–8031. doi:10.1128/MCB.01091-06

Takamizawa, J., H. Konishi, K. Yanagisawa, S. Tomida, H. Osada, H. Endoh, T. Harano, Y. Yatabe, M. Nagino, Y. Nimura, et al. 2004. Reduced expression of the let-7 microRNAs in human lung cancers in association with shortened postoperative survival. *Cancer Res.* 64:3753–3756. doi:10.1158/0008-5472.CAN-04-0637

Thai, T.H., D.P. Calado, S. Casola, K.M. Ansel, C. Xiao, Y. Xue, A. Murphy, D. Frendewey, D. Valenzuela, J.L. Kutok, et al. 2007. Regulation of the germinal center response by microRNA-155. *Science.* 316:604–608. doi:10.1126/science.1141229

Volinia, S., G.A. Calin, C.G. Liu, S. Ambs, A. Cimmino, F. Petrocca, R. Visone, M. Iorio, C. Roldo, M. Ferracin, et al. 2006. A microRNA expression signature of human solid tumors defines cancer gene targets. *Proc. Natl. Acad. Sci. USA.* 103:2257–2261. doi:10.1073/pnas.0510565103

Weng, A.P., A.A. Ferrando, W. Lee, J.P. Morris IV, L.B. Silverman, C. Sanchez-Irizarry, S.C. Blacklow, A.T. Look, and J.C. Aster. 2004. Activating mutations of NOTCH1 in human T cell acute lymphoblastic leukemia. *Science.* 306:269–271. doi:10.1126/science.1102160

Weng, A.P., J.M. Millholland, Y. Yashiro-Ohtani, M.L. Arcangeli, A. Lau, C. Wai, C. Del Bianco, C.G. Rodriguez, H. Sai, J. Tobias, et al. 2006. c-Myc is an important direct target of Notch1 in T-cell acute lymphoblastic leukemia/lymphoma. *Genes Dev.* 20:2096–2109. doi:10.1101/gad.1450406

Whitman, S.P., K. Maharry, M.D. Radmacher, H. Becker, K. Mrózek, D. Margeson, K.B. Holland, Y.Z. Wu, S. Schwind, K.H. Metzeler, et al. 2010. FLT3 internal tandem duplication associates with adverse outcome and gene- and microRNA-expression signatures in patients 60 years of age or older with primary cytogenetically normal acute myeloid leukemia: a Cancer and Leukemia Group B study. *Blood.* 116:3622–3626. doi:10.1182/blood-2010-05-283648

Xiao, C., D.P. Calado, G. Galler, T.H. Thai, H.C. Patterson, J. Wang, N. Rajewsky, T.P. Bender, and K. Rajewsky. 2007. MiR-150 controls B cell differentiation by targeting the transcription factor c-Myb. *Cell.* 131:146–159. doi:10.1016/j.cell.2007.07.021

Zhuang, Y., P. Soriano, and H. Weintraub. 1994. The helix-loop-helix gene E2A is required for B cell formation. *Cell.* 79:875–884. doi:10.1016/0092-8674(94)90076-0